Supporting Information

Role of the Three-Phase Boundary of the Platinum−Support Interface in Catalysis: A Model Catalyst Kinetic Study

Evangelos I. Papaioannou[†,#], *Christoph Bachmann*[‡,#], *Jonas J. Neumeier*[‡], *Daniel Frankel*[†], *Herbert Over*[‡], *Juergen Janek**,[‡], *Ian S. Metcalfe**,[†]

[†]School of Chemical Engineering and Advanced Materials, Newcastle University, Merz Court, Newcastle-upon-Tyne, NE1 7RU, UK

[‡]Institute for Physical Chemistry, Justus-Liebig-University of Giessen, Heinrich-Buff-Ring 17, 35392 Giessen, Germany.

*Correspondence to: Juergen.Janek@phys.Chemie.uni-giessen.de, i.metcalfe@ncl.ac.uk

Characterization

High Resolution Scanning Electron Microscopy (HRSEM)

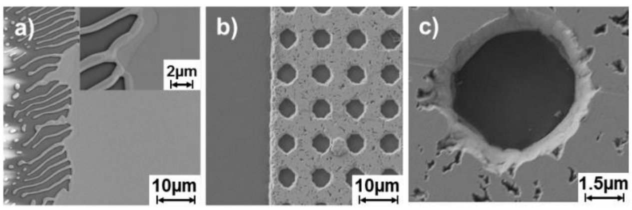

Figure S1. Different steps for structuring the YSZ- and Al_2O_3-supported Pt films by a subtractive lithographic technique. (a) after the ablation and sintering stage the Pt film showed a smooth and dense surface, but the edges of the film had frayed irregular contours, (b-c) after the removal of the resist the Pt edges presented a sharp structure, although the Pt surface had been roughened due to the etching and removal processes (HRSEM micrographs shown here are from sample 16PtYSZ).

Atomic Force Microscopy (AFM)

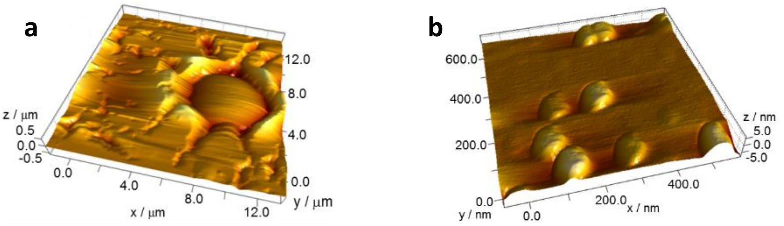

Figure S2. (a) AFM image of a hole and (b) of the base of a hole of sample 1PtYSZ. The AFM topographic image show a Pt wall exhibiting imperfections (a). Of particular interest are nanoscale features approximately 5 nm in height and tens of nanometres laterally (b). These features are most likely irregularities on the YSZ surface due to ion beam bombardment during the etching process.

X-ray Diffraction (XRD)

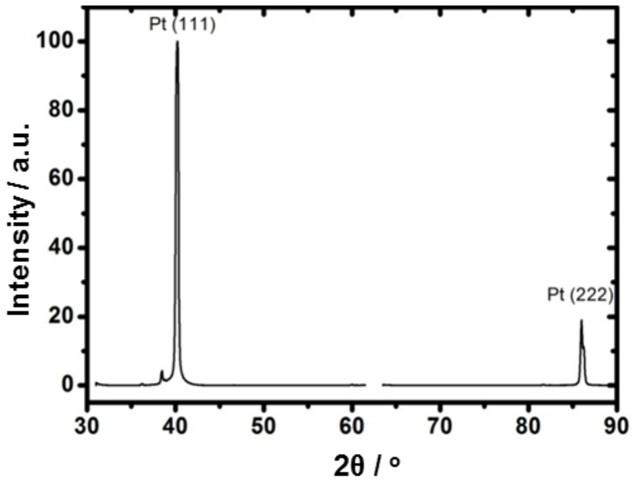

Figure S3. XRD showing that single crystalline (111) orientation dominates the Pt structure for sample 16PtYSZ. A low intensity peak and shoulder to the left of the Pt(111) peak can be attributed to trace amounts of material with argon implanted into the Pt(111) plane. Similar XRD patterns were obtained for all YSZ- and Al_2O_3-supported samples.

Arrhenius plot

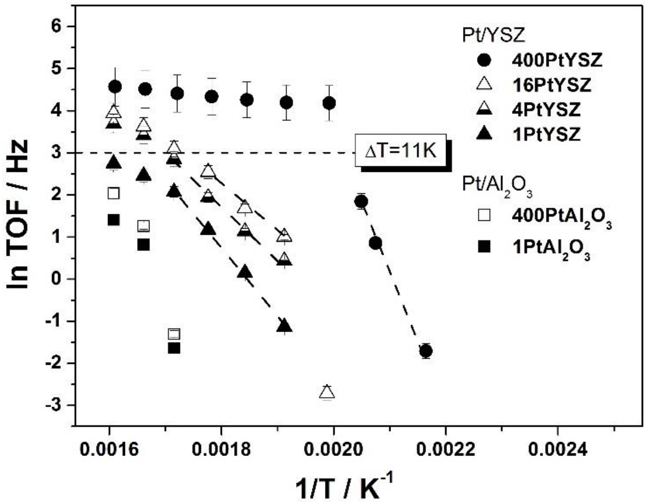

Figure S4. Figure 4 with the lines whose slopes were used to calculate activation energies for the four Pt/YSZ samples.

Table S1. Reported activation energies (E_a) for the CO oxidation over supported and unsupported Pt catalysts.

Catalyst	T (K)	E_a (kJ mol^{-1})	Ref.
Pt(111)	323 - 430	35 - 70	1
Pt(110)	550 - 610	110 ± 10	2
Pt(100)	<400	54	3
Pt(100)	500 - 725	137	3
Pt/Al_2O_3[a]	300 - 800	30 - 125	4
Pt/SiO_2	400 - 450	103	3
Pt/SiO_2	520 - 590	94	5
Pt/SiO_2	500 - 550	98	5
Pt/SiO_2	570 - 660	110 ± 10	2
1PtYSZ	523 - 583	135 ± 5	this work
4PtYSZ	523 - 583	92 ± 6	this work
16PtYSZ	523 - 563	94 ± 8	this work
400PtYSZ	462 - 488	250 ± 40	this work
Pt/CeO_2	420 - 440	63	5
Pt/CeO_2	410 - 440	64	5
Pt/NiO	430 - 490	96	5

Pt/MnO_2	430 - 510	66	5

[a]Various studies.

1. C. Hardacre, R.M. Ormerod, R.M. Lambert, Low-temperature carbon monoxide oxidation on Pt (111). Dependence of apparent activation energy on reactant gas composition, Chem. Phys. Lett. 206 (1993) 171-174.
2. S.M. McClure, M. Lundwall, Z. Zhou, F. Yang, D.W. Goodman, Characterization of Pt/SiO_2 Model Catalysts at UHV and Near Atmospheric Pressures, Catal. Lett., 133 (3) (2009) 298-306.
3. PJ. Berlowitz, C.H.F. Peden, D.W. Goodman, Kinetics of CO Oxidation on Single-Crystal Pd, Pt, and Ir, J. Phys. Chem. 92 (1988) 5213-5221.
4. C. Hardacre, R.M. Ormerod, R.M. Lambert, Low-temperature carbon monoxide oxidation on Pt (111). Dependence of apparent activation energy on reactant gas composition, Chem. Phys. Lett. 206 (1993) 171-174.
5. K. An, S. Alayoglu, N. Musselwhite, S. Plamthottam, G. Melaet, A.E. Lindeman, G.A. Somorjai, Enhanced CO Oxidation Rates at the Interface of Mesoporous Oxides and Pt Nanoparticles, J. Am. Chem. Soc. 135 (44) (2013) 16689-16696.

Experimental

All experiments reported in the manuscript were repeated twice to investigate reproducibility. The measured rates of CO_2 production did not vary more than 15% in all cases during reproducibility experiments.